Bioorganic & Medicinal Chemistry 20 (2012) 3306–3316

Contents lists available at SciVerse ScienceDirect

Bioorganic & Medicinal Chemistry

journal homepage: www.elsevier.com/locate/bmc

Synthesis, biological evaluation and molecular modeling study of pyrazole and pyrazoline derivatives as selective COX-2 inhibitors and anti-inflammatory agents. Part 2

Magda A.-A. El-Sayed [a], Naglaa I. Abdel-Aziz [b,*], Alaa A.-M. Abdel-Aziz [b,c], Adel S. El-Azab [c,d], Kamal E.H. ElTahir [e]

[a] Department of Pharmaceutical Organic Chemistry, Faculty of Pharmacy, University of Mansoura, Mansoura 35516, Egypt
[b] Department of Medicinal Chemistry, Faculty of Pharmacy, University of Mansoura, Mansoura 35516, Egypt
[c] Department of Pharmaceutical Chemistry, College of Pharmacy, King Saud University, Riyadh 11451, Saudi Arabia
[d] Department of Organic Chemistry, Faculty of Pharmacy, Al-Azhar University, Cairo 11884, Egypt
[e] Department of Pharmacology, College of Pharmacy, King Saud University, Riyadh 11451, Saudi Arabia

ARTICLE INFO

Article history:
Received 9 January 2012
Revised 15 March 2012
Accepted 21 March 2012
Available online 29 March 2012

Keywords:
Pyrazole
Pyrazoline
Synthesis
COX-2 inhibitors
Anti-inflammatory
Molecular modeling

ABSTRACT

New pyrazole and pyrazoline derivatives have been synthesized and their ability to inhibit ovine COX-1/COX-2 isozymes was evaluated using in vitro cyclooxygenase (COX) inhibition assay. Among the tested compounds, *N*-((5-(4-chlorophenyl)-1-phenyl-3-(trifluoromethyl)-1*H*-pyrazol-4-yl)methylene)-3,5-bis(trifluoromethyl)aniline **8d** exhibit optimal COX-2 inhibitory potency (IC_{50} = 0.26 lM) and selectivity (SI) = >192.3] comparable with reference drug celecoxib (IC_{50} value of 0.28 lM and selectivity index of 178.57). Moreover, the anti-inflammatory activity of selected compounds, which are the most selective COX-2 inhibitors in the COX inhibition assay, was investigated in vivo using carrageenan-induced rat paw edema model. Molecular modeling was conducted to study the ability of the active compounds to bind into the active site of COX-2 which revealed a similar binding mode to SC-558, a selective COX-2 inhibitor.

1. Introduction

Inflammation is a normal response to any noxious stimulus that threatens the host and may vary from a localized response to a generalized one.[1] Non-steroidal anti-inflammatory drugs (NSAIDs) are widely used for the treatment of rheumatism diseases, as rheumatoid arthritis, and pain.[2,3] NSAIDs achieve their anti-inflammatory action through an inhibitory effect on cyclooxygenase enzyme (COX), a protein essential for prostaglandin biosynthesis from arachidonic acid. COX exists under two isoforms, namely COX-1 and COX-2. In general terms, COX-1 is responsible for protecting the gastric mucosa and maintaining homeostasis, whereas COX-2 is induced by proinflammatory stimuli at the inflammatory sites.[4–6] Gastrointestinal (GI) irritation, bleeding and ulceration side effects are associated with long term use of the classical NSAIDs due to high COX-1 versus COX-2 selectivity.[2,7,8] Thus, it is reasonable to speculate increasing the specificity for COX-2 over COX-1 is one of the strategies that could be employed to improve safety profile and therapeutic potency of NSAIDs. The improved safety profile of COX-2 inhibitors may allow the use of these new agents for long-term prophylactic use in certain chronic diseases.[9–11] This has led intense efforts in search for potent and selective COX-2 inhibitors which could provide anti-inflammatory drugs with fewer risks.[12–16] Research attempts in the discovery of selective COX-2 inhibitors have produced many diarylheterocycles and central ring pharmacophore templates (Fig. 1).[12–14] However, the recent success of pyrazole-based COX-2 inhibitors has highlighted the importance of these heterocycles in medicinal chemistry.[12] Several classes of compounds having selective COX-2 inhibitory activity have been reported in the literature such as SC-558[17] and celecoxib[18] (Fig. 1, A and B, respectively).

Thus our main objective is to design novel cyclic imides as specific inhibitors of COX-2 in the hope that these molecules may be further explored as powerful and novel non-ulcerogenic anti-inflammatory lead-candidates. Our strategy is intended to obtain potent anti-inflammatory activity with selective inhibition of COX-2 using traditional medicinal chemistry techniques motivated by the comparative modeling of a COX-1 and -2 complexed with **A** and **B** together with the available pharmacophore. We have recently studied a series of arylhydrazone and 1,5-diphenylpyrazole

* Corresponding author. Tel./fax: +20 502247496.
E-mail address: naglaabdalaziz2005@yahoo.com (N.I. Abdel-Aziz).

0968-0896/$ - see front matter © 2012 Elsevier Ltd. All rights reserved.
http://dx.doi.org/10.1016/j.bmc.2012.03.044

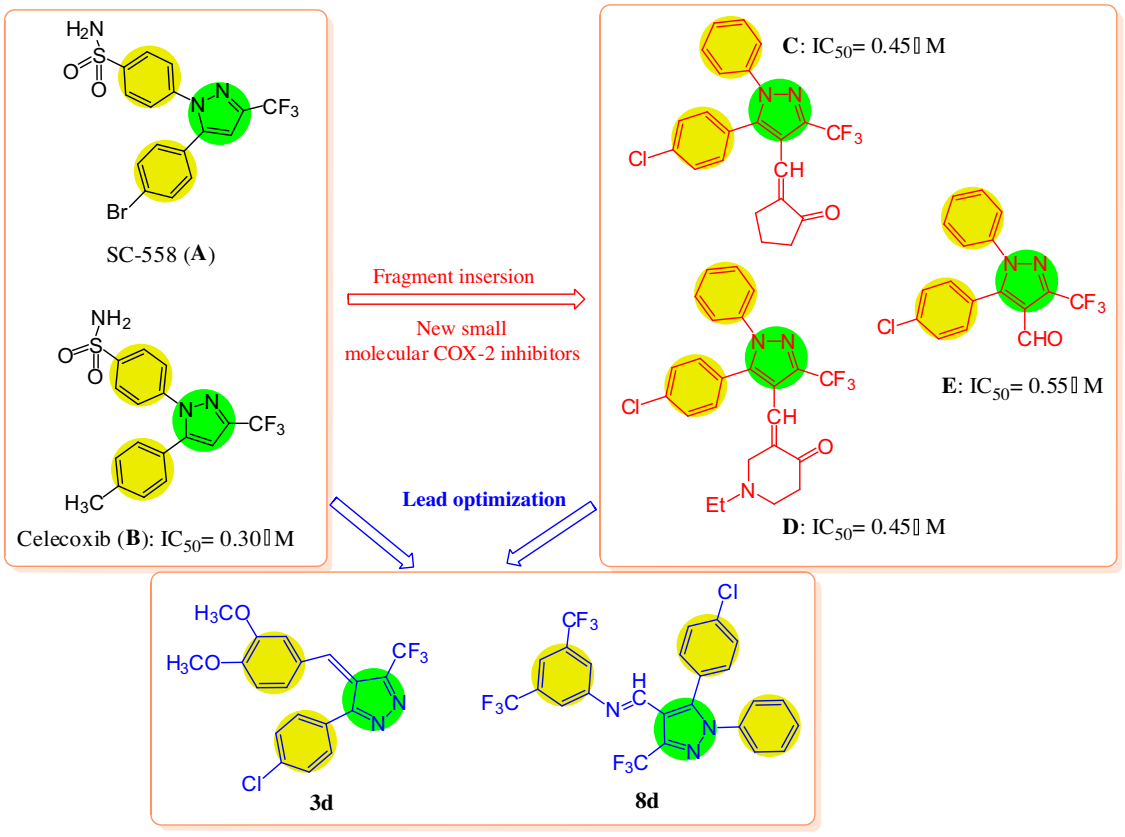

Figure 1. Representative examples of selective COX-2 inhibitors (**A**–**E**) the designed pyrazoles (**3d** and **8d**).

derivatives which were evaluated for their anti-inflammatory and COX-2 inhibitory activities (Fig. 1).[19] Continuing our studies on pyrazole derivatives as attractive candidates as anti-inflammatory agents and COX-2 inhibitors we have designed a number of new pyrazole and pyrazoline derivatives and biologically evaluated their in vitro COX-1/COX-2 and in vivo assessment as anti-inflammatory activities (Fig. 1). Drug-likeness and molecular docking methodology were used to identify the structural features required for the COX-2 inhibition properties of these new series. The results of this molecular docking could support the postulation that our active compounds may act on the same enzyme target where COX-2 inhibitors act confirming the molecular design of the reported class of COX-2 inhibitors.

2. Results and discussion

2.1. Chemistry

The synthetic route used to synthesize the target compounds is outlined in Schemes 1–3.

2.1.1. Synthesis of compounds 1–5 (Scheme 1)

Claisen condensation of *p*-chloroacetophenone with ethyl trifluoroacetate provided trifluoromethyl-1,3-dicarbonyl adduct **1** in a good yield. Interaction between compound **1** and different aldehydes in ethanolic sodium hydroxide afforded the corresponding chalcone derivatives **2a**–**f**. The β-diketone moieties in the later compounds were reacted with hydrazine hydrate in refluxing ethanol affording the corresponding pyrazole derivatives **3a**–**f**. The spectral and microanalytical data for compounds **2,3a**–**f** were consistent with their chemical structures. Moreover, alkylation of active methylene compounds is a very important transformation in organic synthesis. Anhydrous ferric chloride has been emerged as a powerful lewis acid catalyst for C–C bond formation between active methylene compound and alcohol since direct substitution of the hydroxyl group is difficult due to its poor leaving ability.[20] Hence, reaction of β-diketone **1** with benzyl alcohol was performed in dichloromethane in the presence of catalytic amount of anhydrous ferric chloride to afford compound **4.** Cyclocondensation of the later compound with hydrazine hydrate in refluxing ethanol afforded the corresponding pyrazole derivative **5**.

The structures of the prepared compounds were substantiated by elemental and spectral analyses. For example, the structure of compound **5** was confirmed by IR data which exhibited absorption bands at 3200, 3096 cm^{-1} (NH) and 1610, 1590 cm^{-1} (C=C, C=N) and no absorption bands for (C=O). The ^{1}H-NMR spectra of compound **5** showed the methylene of the benzyl group and NH at 4.2 and 14.10 ppm, respectively.

2.1.2. Synthesis of compounds 6–9 (Scheme 2)

Cyclocondensation of phenylhydrazine with trifluoromethyl-1,3-diketone **1** afforded the corresponding 1,5-diphenyl pyrazole derivative **6** as the major product. The NH_2 in phenylhydrazine is more nucleophilic than NH and would react preferentially with the more reactive carbonyl group ($COCF_3$) leading to the production of 1,5-diphenyl pyrazole regioisomer as a major product specially if the reaction is carried out in acidic medium.[18] Vilsmeier formylation of 1,5-diphenyl pyrazole derivative **6** provided the corresponding aldehyde **7** which reacted with different substituted aromatic amines affording the corresponding Schiff bases **8a**–**d** in a good yield. In addition, Knoevenagel condensation of compound **7** with malononitril in DMF and sodium acetate gave compound **9**. The structures of the isolated products **8a–d** and **9** were estab-

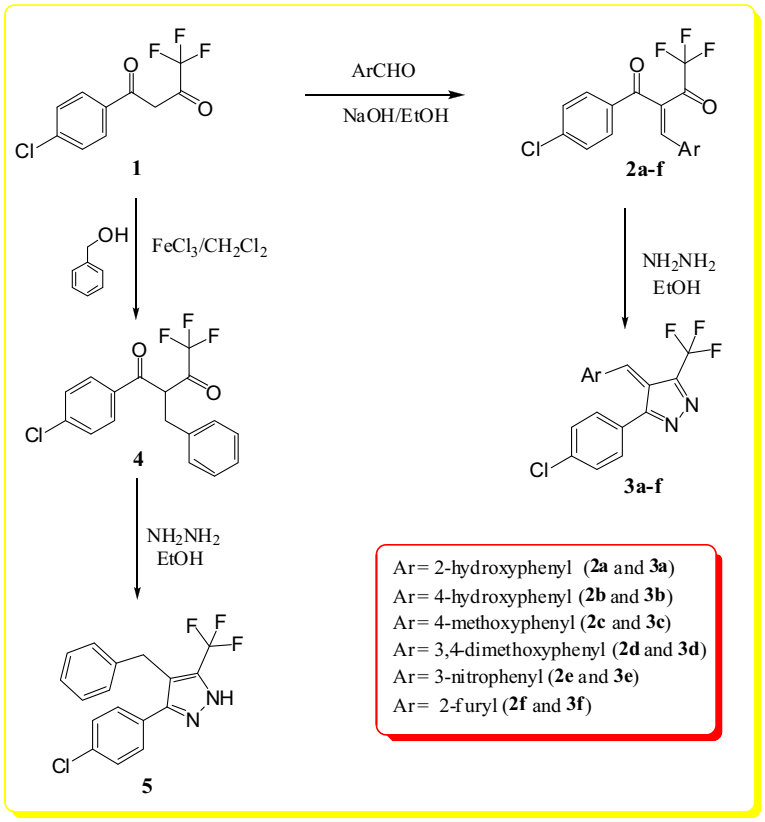

Scheme 1. Synthesis of diarylpyrazole derivatives (**3** and **5**).

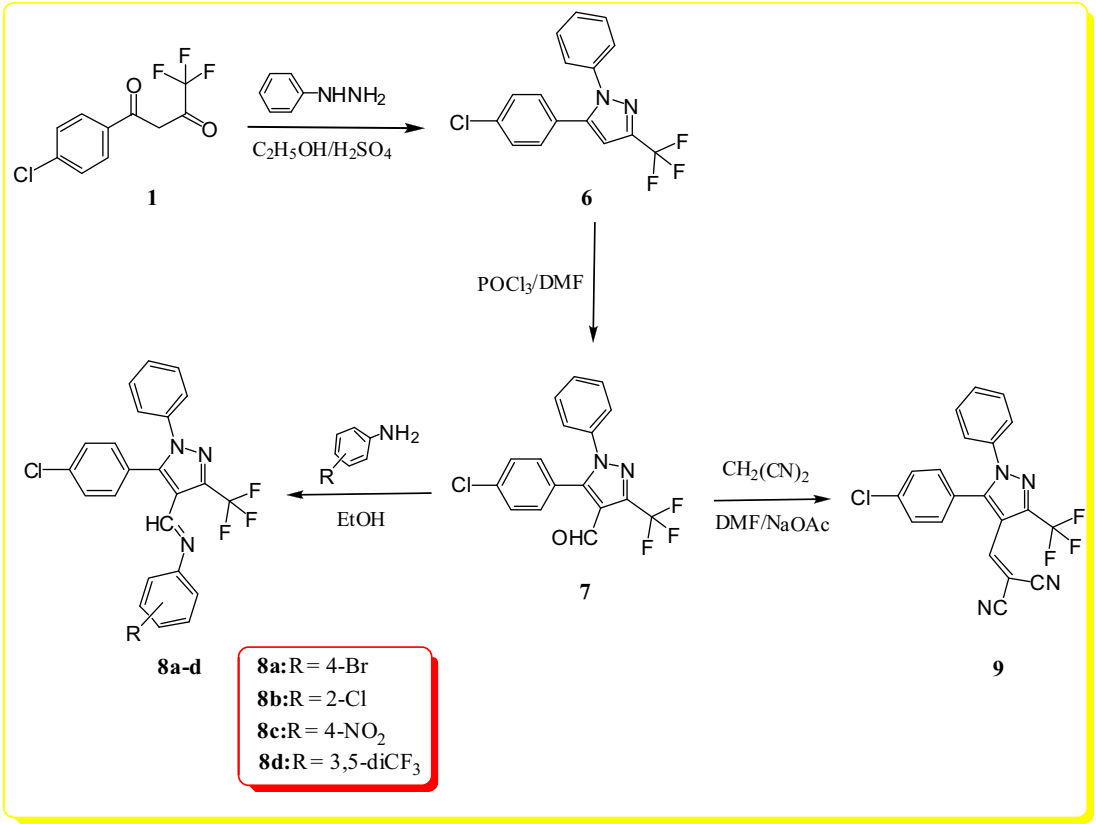

Scheme 2. Synthesis of triarylpyrazole derivatives (**8** and **9**).

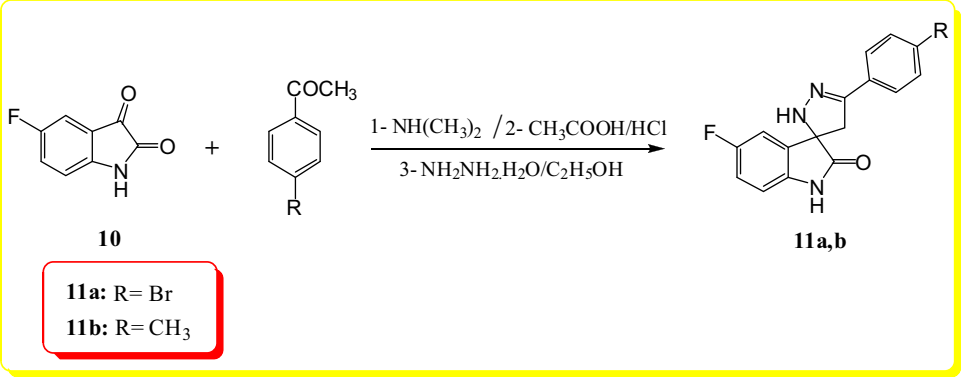

Scheme 3. Synthesis of spiropyrazoline derivatives (**11**).

lished on the basis of their elemental and spectral analyses. IR data for compound **9** exhibited characteristic absorption bands at 2211, 2205 (CN).

2.1.3. Synthesis of compounds 11a,b (Scheme 3)

Crossed aldol condensation between isatin and acetophenone derivatives was reported to be achieved in the presence of dimethylamine as a basic catalyst followed by dehydration to give the corresponding chalcones.[21] Nucleophilic Michael addition of hydrazine hydrate to the later compounds gave spiropyrazolines.[22–25] Moreover, spiropyrazolines were prepared in a good yield via a one-pot synthesis without the isolation of the intermediate chalcones.[25,26] Hence, in this work, fluoroisatin reacted with acetophenone derivatives in the presence of dimethylamine for 30 min at room temperature and the formed solid was treated with glacial acetic acid and hydrochloric acid for another 30 min at 80 °C. Hydrazine hydrate was then added to the previous acidic solution to give the corresponding spiropyrazoline derivatives **11a,b**. The structures of the final products were established by physical and spectral methods.

2.2. Biological evaluation

2.2.1. In vitro cyclooxygenase (COX) inhibition assay

It was found that the structurally simple compounds, pyrazoles (Fig. 1, A–D), were obtained as a potent COX-2-selective inhibitor. According to the previous rational, the compounds synthesized in this work were evaluated for their ability to inhibit COX-1 and COX-2 using an ovine COX-1/COX-2 assay kit (Catalog No. 560101, Cayman Chemicals Inc., Ann Arbor, MI, USA) according to the protocol recommended by the supplier. IC_{50} (μM) are determined as the means of two determinations acquired and the deviation from the mean is <10% of the mean value. The selectivity index (SI values) was defined as IC_{50}(COX-1)/IC_{50}(COX-2). In the assay system, the IC_{50} values of celecoxib on COX-1 and COX-2 were determined to be >50 and 0.28 μM, respectively indicating that celecoxib is a selective COX-2 inhibitor. None of the tested compounds showed inhibitory activity on COX-1 down to 50 μM. Some of the tested compounds (**2d**, **3b**, **3d**, **3e**, **8c** and **8d**) were found to be potent and selective similar to celecoxib against COX-2. IC_{50} values in μM (Table 1) acquired by determination of the in vitro ability of the tested compounds to inhibit COX-2 showed that compound **8d** with 3,5-ditrifluoromethyl substituents on the C4-phenyl ring was more potent and selective COX-2 inhibitor (IC_{50} = 0.26 μM, SI = >192.3) compared with the reference drug celecoxib (IC_{50} = 0.28 μM, SI = >178.57). Despite, COX-2 potency and selectivity were increased in the cyclized derivatives **3** relative to the corresponding chalcones **2**, compound **3f** had less potency and selectivity compared with compound **2f**. It was also noticed that replacement of the phenyl ring in compounds **2b–e** and **3b–e** with a furyl one as in compounds **2f** and **3f** led to dramatic decrease in the COX-2 activity. In addition, replacement of the benzylidene fragment with a benzyl moiety abolishes the COX-2 activity as in compound **5**. Moreover, no activity was observed for the spiropyrazoline compounds containing isatin moiety (**11a** and **11b**).

Table 1
Data of the *in vitro* COX-1/COX-2 enzyme inhibition assay of the designed compounds

Compd No.	IC_{50}[a] (μM)		SI[c]
	COX-1[b]	COX-2	
2a	>50	46.0	>1.09
2b	>50	1.2	>41.67
2c	>50	3.3	>15.15
2d	>50	0.50	>100.00
2e	>50	0.66	>75.76
2f	>50	40.2	>1.24
3a	>50	44.4	>1.13
3b	>50	0.48	>104.17
3c	>50	2.1	>23.81
3d	>50	0.29	>172.41
3e	>50	0.43	>116.28
3f	>50	48.0	>1.04
5	>50	>50	>1.00
8a	>50	3.2	>15.63
8b	>50	49.0	>1.02
8c	>50	0.41	>121.95
8d	>50	0.26	>192.31
9	>50	>50	>1.0
11a	>50	>50	>1.0
11b	>50	>50	>1.0
Diclofenac	0.22	3.1	0.07
Celecoxib	>50	0.28	>178.57

[a] IC_{50} value is the compound concentration required to produce 50% inhibition of COX-1 or COX-2 for means of two determinations and deviation from the mean is <10% of the mean value.
[b] No inhibition of COX-1 up to 50 μM.
[c] Selectivity index (COX-1 IC_{50}/COX-2 IC_{50}).

2.2.2. In vivo anti-inflammatory studies

Anti-inflammatory activity of eleven compounds, which showed the highest specificity for COX-2 enzyme in the in vitro assay including compounds **2b–e**, **3b–e**, **8a**, **8c** and **8d** was evaluated by employing the well-known rat carrageenan-induced foot paw edema model (Table 2). The percentages of edema reduction given by the tested compounds, diclofenac sodium and celecoxib, as a reference drugs, are depicted in Table 2. Moreover, ED_{50} was measured after 2 h of treatment with carrageenan at which maximum percentage of inhibition of carrageenan-induced edema was reached. All of the ED_{50} values were determined using three doses

Table 2
Data of the in vivo anti-inflammatory activity of the designed compounds against carrageenan-induced rat paw edema (IP)

Compd No.	% Inhibition of edema[a]		ED_{50}[c]	
	100 mg/kg	200 mg/kg	mg/kg	mmol/kg
2b	39.2	78.9	130 ± 7.5	0.366
2c	26.3	52.4	195 ± 11.3	0.528
2d	38.7	80.2	128 ± 6.3	0.321
2e	37.9	80.0	132 ± 9.1	0.343
3b	35.3	81.4	130 ± 7.9	0.370
3c	33.4	69.1	148 ± 8.1	0.405
3d	42.0	88.7	118 ± 4.9	0.298
3e	37.6	84.5	121 ± 6.7	0.318
8a	25.2	61.1	170 ± 79.9	0.335
8c	43.7	86.7	115 ± 6.1	0.243
8d	52.0	89.3	96 ± 4.3	0.170
Diclofenac[b]	48.7	87.3	63 ± 7.5	0.198
Celecoxib[c]	57.0	83.0	70.4 ± 0.8	0.185

[a] The results are expressed as means ± SEM (n = 4–6) after 2 h following IP of the test compounds.
[b] Values are determined at 50 and 100 mg/kg IP.
[c] ED_{50} was the effective dose calculated after 2 h.

of 50, 100 and 200 mg/kg in the test compounds and 25, 50 and 100 mg/kg in the reference drugs diclofenac and celecoxib. Out of 11 compounds, 10 compounds (**2b**, **2d**, **2e**, **3b–e**, **8a**, **8c** and **8d**) were found to possess potent anti-inflammatory activity (61–89% reduction in inflammation). Compound **8d** showed the highest anti-inflammatory activity among the tested compounds with ED_{50} of 0.170 mmol/kg and the rest of compounds showed ED_{50} in the rang of 0.243–0.528 mmol/kg, as compared to diclofenac and celecoxib (ED_{50} = 0.198 and 0.185 mmol/kg, respectively).

2.3. Molecular calculation and results

Modeling studies are required in order to construct molecular models that incorporate all experimental evidence reported.[27,28] These models are necessary to obtain a consistent and more precise picture of the biological active molecules at the atomic level and furthermore, provide new insights that can be used to design novel therapeutic agents.[15,19]

2.3.1. ADME profiling

The bioavailability of the most active compounds **2b**, **2d**, **2e**, **3b**, **3d**, **3e**, **8c** and **8d** and the reference drug celecoxib was assessed using ADME (absorption, distribution, metabolism and elimination; http://www.molinspiration.com/cgi-bin/properties) prediction methods. In particular, we calculated the compliance of compounds to the Lipinski's rule of five.[29] This approach has been widely used as a filter for substances that would likely be further developed in drug design programs. Briefly, this simple rule is based on the observation that most orally administered drugs have a molecular weight ≤500, a log$P$≤5, hydrogen bond donor sites ≤5 and hydrogen bond acceptor sites (N and O atoms) ≤10. In addition, we calculated the total polar surface area (TPSA) since it is another key property that has been linked to drug bioavailability. Thus, passively absorbed molecules with a TPSA >140 are thought to have low oral bioavailability. Molecules violating more than one of these rules may have problems with bioavailability. Predictions of ADME properties for studied compounds (Supplementary data) showed that compounds (**2b**, **2d**, **2e**, **3b**, **3d**, **3e** and **8c**) fulfilled this rule, similarly to clinically used drugs (i.e., celecoxib). Compound **8d** was violated from the rule of five by two represented by molecular weight and log$P$ values. Theoretically, these compounds should present good passive oral absorption and differences in their bioactivity can not be attributed to this property.

2.3.2. 2D-QSAR study

The COX-2 inhibition of the twenty tested compounds, presented in $-\log 1/IC_{50}$ (Table 3), were used in the 2D-QSAR studies using VLife Molecular Design Suite.[30] Compounds were divided in training and test set. This was achieved by setting aside four compounds as test set which have regularly distributed activity. Selection of molecules in the training set and test is a key and important feature of any QSAR model. Therefore the care was taken in such a way that biological activities of all compounds in test set lie within the maximum and minimum value range of biological activities of training set of compounds. A Uni-Column statistics for training set and test set were generated to check correctness of selection criteria for trainings and test set molecules. The maximum and minimum value in training and set were compared in a way that:

1. The maximum value of $-\log 1/IC_{50}$ of test set should be less than or equal to maximum value of $-\log 1/IC_{50}$ of training set.
2. The minimum value of $-\log 1/IC_{50}$ of test set should be higher than or equal to minimum value of $-\log 1/IC_{50}$ of training set.

This observation showed that test set was interpolative and derived within the minimum–maximum range of training set. The mean and standard deviation of $-\log 1/IC_{50}$ values of sets of training and test provide insights to relative difference of mean and point density distribution of two sets. 2D-QSAR models were generated for training set of 16 compounds using multiple linear regression (MLR) method. The best QSAR model was selected on the basis of value of statistical parameters like r^2 (square of correlation coefficient for training set of compounds), q^2 (cross validated r^2), and pred_r^2 (predictive r^2 for the test set of compounds). All QSAR model was validated and tested for its predictability using an external test set of 4 compounds. Statistical results generated by 2D-QSAR analysis showed that QSAR models have good internal as well as external predictability. The results obtained for actual and predicted activity are presented in Table 3 and the residuals were found to be minimal (Table 3, Fig. 2). The regression equation obtained for the different series of compounds is given below.

2D-QSAR model for COX-2 inhibition in $-\log 1/IC_{50}$

$$\begin{aligned} -\mathrm{Log}1/IC_{50} &= -6.1502(\pm 0.9175)\mathrm{SssNHcount} \\ &\quad + 0.7191(\pm 0.0576)\mathrm{T\_N\_N\_4} \\ &\quad + 0.2439(\pm 0.0421)\mathrm{T\_O\_F\_7} + 20.4400n \\ &= 16\ r^2 = 0.8301\ q^2 = 0.7416\ F-\mathrm{test} \\ &= 27.9176\ r^2\mathrm{se} = 0.3315\ q^2\mathrm{se} = 0.4322\ \mathrm{pred}\_r^2 \\ &= 0.8633\ \mathrm{pred}\_r^2\mathrm{se} = 0.3346 \end{aligned}$$

A brief idea of statistical result of 2D-QSAR models, the requirement of different physicochemical parameters and their contributions (positive or negative influence on biological activity), required for potential antibacterial activity was obtained. The regression equation so obtained will be useful for the prediction of biological activities of the designed series of compounds, in future. The QSAR model generated is a tri-parametric model and the statistical best model for COX-2 inhibition ($-\log 1/IC_{50}$) with a coefficient of determination (r^2) = 0.8301 was considered, as the model showed an internal predictive power (q^2 = 0.7416) of 74% and a predictivity for the external test set (pred_r^2 = 0.8633) of about 86%. The low standard error of r^2_se = 0.3315 demonstrates accuracy of the model. The F-test value of 27.9176 shows the overall statistical significance level to be 99.99% of the model, which means that the probability of failure for model is 1 in 10,000.

Table 3
Observed, predicted COX-2 inhibition activity ($-\log 1/IC_{50}$) and residual values of the designed compounds

Compd No.	$-\log 1/IC_{50}$		
	Observed	Predicted	Residual
2a	1.66	1.65	0.01
2b	0.08	0.42	−0.34
2c	0.52	−0.20	0.77
2d	−0.30	−0.42	0.12
2e	−0.18	0.01	−0.19
2f	1.60	1.38	0.22
3a	1.65	1.66	−0.01
3b	−0.32	−0.19	−0.13
3c	0.32	0.43	−0.11
3d	−0.54	−0.43	−0.11
3e	−0.37	0.01	−0.38
3f	1.68	1.41	0.27
5	1.70	1.77	−0.07
8a	0.51	0.78	−0.27
8b	1.69	1.22	0.47
8c	−0.39	−0.18	−0.21
8d	−0.59	−0.24	−0.35
9	1.70	1.59	0.11
11a	1.70	0.98	0.72
11b	1.70	1.60	0.10

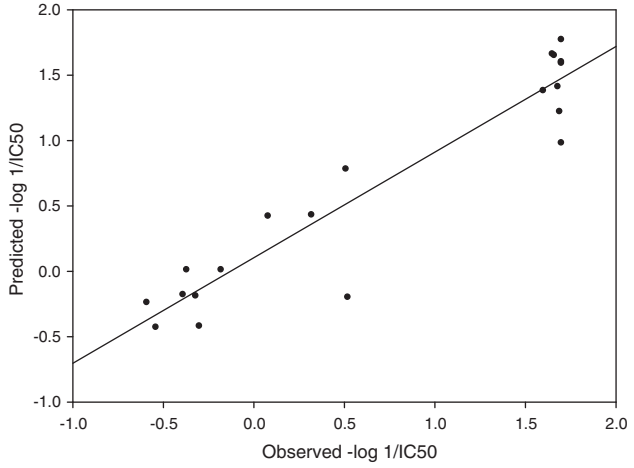

Figure 2. Plot between observed and predicted COX-2 inhibition of the compounds in the training set and test set for the linear regression developed model.

The model is validated by α_ran_$r^2 = 0.001$, α_ran_$q^2 = 0.01$, α_ran_ pred_$r^2 = 0.01$. The randomization test suggests that the developed model have a probability of less than 1% that the model is generated by chance.

The positive coefficients (36.00%) of T_N_N_4 (count of number of Nitrogen atoms separated from any other Nitrogen atom by four bonds) and (15.5%) of T_O_F_7 (count of number of Oxygen atoms separated from any other fluorine atom by seven bonds) showed that increase in the values of this descriptor is beneficial for the COX-2 inhibition activity (like in compounds **2d**, **2e**, **3d**, **3e** and **8c**, **8d**). The next descriptor SssNHcount is a descriptor defines the total number of –NH group connected with two single bonds, indicates a negative contribution to the biologic activity (like in compounds **5**, **11a** and **11b**).

2.3.3. Docking studies

The level of COX-2 inhibition and anti-inflammatory activities of compounds **3d**, **11a** and **8d** prompted us to perform molecular docking studies to understand the ligand–protein interactions in detail. As it is clear from X-ray crystal structure data,[31,32] the COX-2 binding site possesses an additional 2°-pocket that is absent in COX-1, which is highly relevant to the design of selective COX-2 inhibitors. This COX-2 2°-pocket arises due to a conformational change at Tyr^{355} that is attributed to the presence of Ile^{523} in COX-1 relative to Val^{523} having a smaller side chain in COX-2.[31] It has also been reported that replacement of His^{513} in COX-1 by Arg^{513} in COX-2 plays a key role with respect to the H-bond network in the COX-2 binding site. Access of ligands to the 2°-pocket of COX-2 is controlled by histidine (His^{90}), glutamine (Gln^{192}), and tyrosine (Tyr^{355}).[33] Interaction of Arg^{513} with the bound drug is a requirement for time dependent inhibition of COX-2.[34]

All the docking calculations were performed using MOE 2008.10 software installed on 2.0G Core 2 Duo.[15,19,35,36] The crystal structures of COX-2 enzymes complexed with SC-558 [6COX] were used for the docking.[17] The active site of the enzyme was defined to include residues within a 10.0 Å radius to any of the inhibitor atoms. The automated docking program of MOE 2008.10 was used to dock compounds **3d**, **11a** and **8d** on the active sites of COX-2 enzymes (Fig. 2). The most stable docking model was selected according to the best scored conformation predicted by the MOE scoring function. The complexes were energy-minimized with a MMFF94 force field[37] till the gradient convergence 0.05 kcal/mol was reached. The docking energies of −40.36, −5.01 and −43.68 kcal/mol were obtained for **3d**, **11a** and **8d**, respectively (Fig. 3). The compounds **3d** and **8d** could dock into the active site of COX-2 successfully (Fig. 3). Compounds **3d** and **8d** produces a deep moving into the hydrophilic pocket of COX-2. 3,5-di-triflouromethyl fragment of compound **8d** was able to reach the hydrophilic pocket and is involved in classical hydrogen bonding with Gln^{192} (2.61, 2.93 Å) and Arg^{513} (1.85, 2.14 Å). Such interactions are almost essential for COX-2 inhibitory activity, as exemplified by the binding interaction of SC-558, an analogue of celecoxib cocrystallized in the COX-2 active site.[17] Moreover trifluoropyrazole core formed additional three hydrogen bonding with Tyr^{355} (2.09 Å) and Arg^{513} (2.98, 3.29 Å) while 4-chlorophenyl moiety showed weak interaction with amino acid residue Trp^{387} (2.92 Å). In addition; such interaction forces the triarylpyrazole core to adopt a specific orientation at the top of the channel. This moiety is involved in hydrophobic interaction with Trp^{387}, Tyr^{385}, Val^{523}, Ala^{527} and Phe^{518}. The lateral pocket of COX-2 would therefore be responsible for the COX-2 selectivity of **8d** and contributed to stabilize the ligand–enzyme complexes (Fig. 3). Similarly compound **3d** was modeled in the active site of COX-2 enzyme (Fig. 3). The dimethoxy fragment of **3d** is able to reach the hydrophilic pocket and is involved in hydrogen bonding forming a three hydrogen bonding interaction with His^{90} (3.07, 2.56 Å) and Gln^{192} (2.97 Å). Moreover trifluoropyrazole core of compound **3d** formed additional three hydrogen bonding with Tyr^{355} (2.56, 3.20 Å) and Arg^{120} (2.76, 3.34 Å). In a similar manner of compound **8d**, 4-chlorophenyl moiety of **3d** is involved in hydrophobic interaction with Trp^{387}, Tyr^{385}, Val^{523}, Ala^{527} and Phe^{518}. The complex generated by docking studies of **8d** with COX-2 and superimposition with the structure of the selective inhibitor, SC-558, co-crystallized with COX-2, illustrated in Figure 3, shows that compound **8d** can bind in the active site of this enzyme in approximately similar fashion as the pyrazolic prototype (SC-558) with additional hydrogen bonds. Additionally, 3,5-di-triflourophenyl system are positioned in the same region as *p*-sulfonamido-phenyl ring of SC-558, while, the 4-chlorophenyl fragment of compound **8d** is close to the *p*-Br-phenyl ring of SC-558, in the aromatic region of the active site lined by aromatic amino acid residues such as Phe^{518}, Tyr^{385} and Trp^{387}, among others. In short, the described interactions are typical of selective inhibitors of COX-2, confirming the molecular design of the reported class of anti-inflammatory pyrazole derivatives.[38,39]

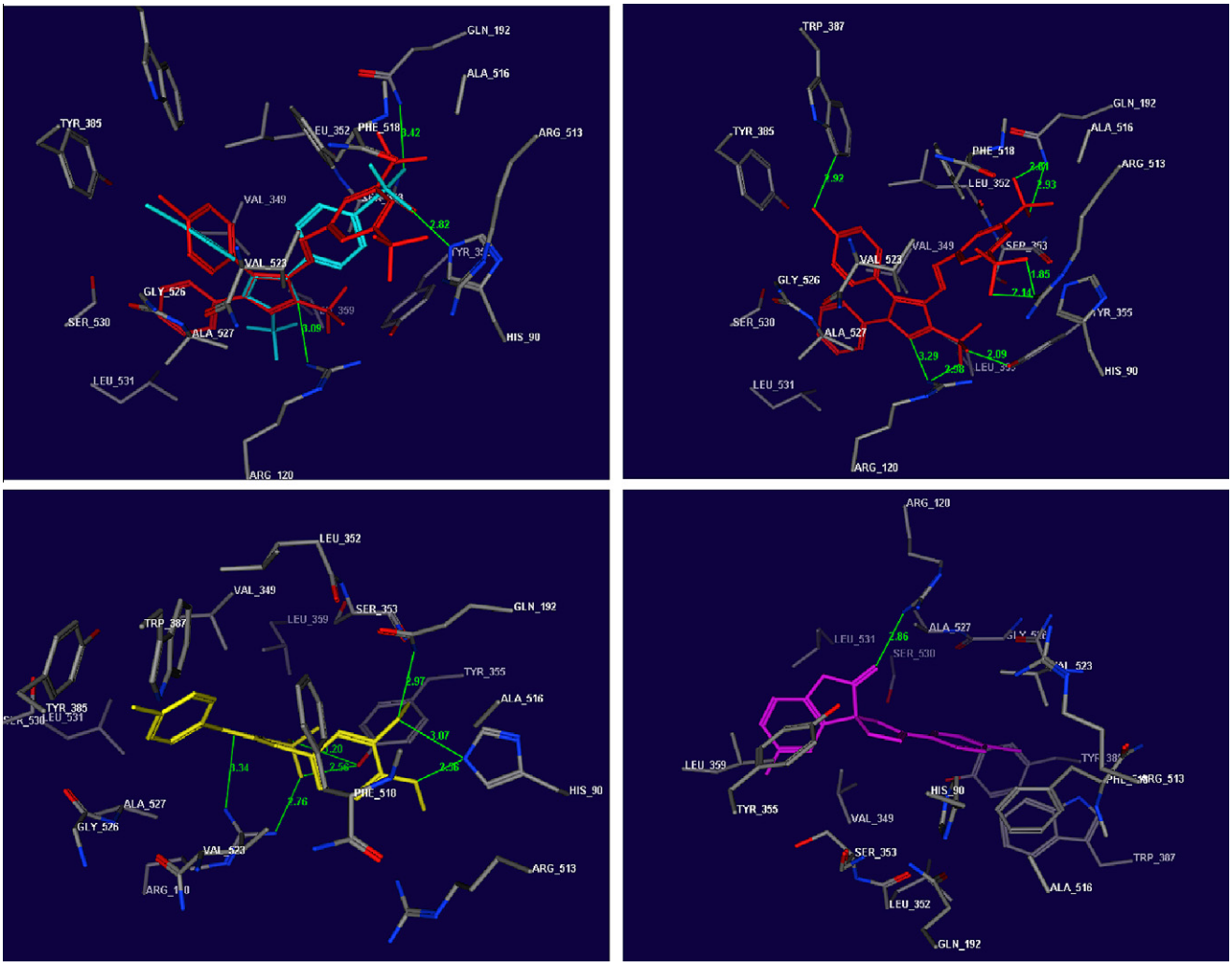

Figure 3. Orientation of **8d** (color red) in COX-2 active pocket (Upper left panel; SC-558 is shown as cyan). Docking of compounds **8d** (Upper right panel), **3d** (Lower left panel) and **11a** (Lower right panel) into the active site of COX-2. Hydrogen bonds are shown in green.

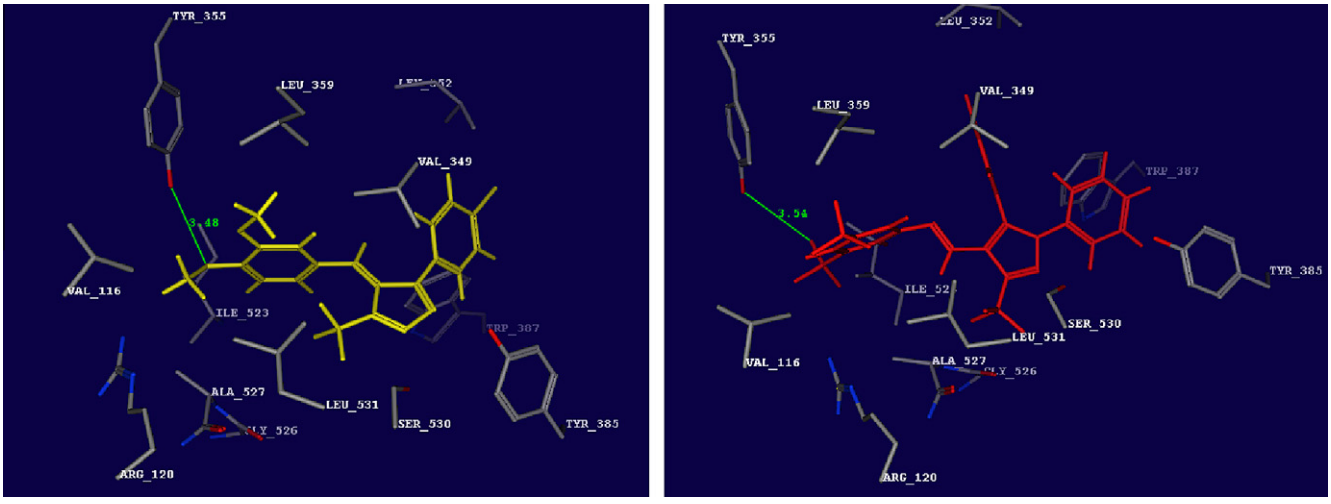

Figure 4. Docking of compounds **3d** (left panel) and **8d** (right panel) into the active site of COX-1. Hydrogen bonds are shown in green.

The lower interaction energy observed for **11a** rationalizes the insufficient binding of spiropyrazoline core into the COX-2 active site than that of the pyrazole core of **8d** (Fig. 3). The insufficient binding can be explained in terms of the occurrence of only one hydrogen bond between the carbonyl group and Arg^{120} (2.86 Å) and the absence of hydrogen bonding with Gln^{192}, His^{90} and Arg^{513} which is essential for COX-2 inhibitory activity.

On the other hand, compounds **3d** and **8d** as representative examples were docked into the active site of COX-1 enzyme to understand the inactivity of such compounds toward COX-1 inhibition (Fig. 4). The crystal structures of COX-1 enzymes complexed with flurbiprofen[40] [1EQH] were used for the docking using the same protocol described above. The two compounds could dock into the active site of COX-1 successfully. The binding energies of −4.22 and −7.67 kcal/mol were obtained for **3d** and **8d**, respectively (Fig. 3). The insufficient binding of both compounds can be explained in terms of the occurrence of very weak hydrogen bonds in which the 3,4-dimethoxyphenyl group of compound **3d** formed such weak bonds with Tyr^{355} (3.48 Å) while 3,5-diCF_3phenyl group of compound **8d** formed similar weak bonds with Tyr^{355} (3.54 Å). The hydrophobic phenyl rings of **3d** and **8d** were surrounded by active site amino acid residues Tyr^{385}, Val^{349}, Trp^{387} and Ser^{530}.

3. Conclusion

Pyrazole and pyrazoline derivatives were synthesized and screened for COX-1/COX-2 inhibition and anti-inflammatory activity. Compounds which showed significant COX-2 inhibition were subjected to anti-inflammatory studies. Compound **8d** exhibit optimal COX-2 inhibitory potency (IC_{50} = 0.26 μM) and selectivity (SI) = >192.3] comparable with celecoxib, so it appears promising. Various physicochemical indices are helpful for the understanding of COX-2 inhibition results, as shown by our 2D-QSAR study. The 2D-QSAR results could not be addressed to a concrete drug–receptor interaction, but they can reveal trends in the relationship between ligand structures and their activities for our set of COX-2 inhibitors. Analysis of 2D-QSAR models provides details on the fine relationship linking structure and activity and offers clues for structural modifications that can improve the activity. These trends should prove to be an essential guide for the future work. Molecular docking studies further help in understanding the various interactions between the ligands and enzyme active sites in detail and thereby help to design novel potent inhibitors. It is clear that the trifluoromethyl moieties of **8d** inserts deep inside the COX-2 2°-pocket and forming strong hydrogen bond with Gln^{192} (2.61, 2.93 Å) and Arg^{513} (1.85, 2.14 Å). This result was corroborated by molecular docking studies with COX-2 inhibition, which showed that this compound presents the pharmacophoric requisites for COX-2 inhibition. Indeed molecular docking studies further supported the strong inhibitory activity of **8d** and further help understanding the various interactions between the ligands and enzyme active sites in detail and thereby help to design novel potent inhibitors. The structure–activity relationships acquired show that appropriately substituted triarylpyrazole have the necessary geometry to provide potent and selective inhibition of the COX-2 isozyme, and to exhibit excellent anti-inflammatory activities. Furthermore analysis of the predicted ADME properties for newly prepared compounds opens the possibility for further optimization of studied compounds. Compound **8d** is found to be too lipophilic due to the larger number of trifluoromethyl fragment; therefore, it could serve as lead molecule for further optimization of both specific biological activity and ADME properties.

4. Experimental

4.1. General

Melting points was determined using Fisher-Johns melting point apparatus and are uncorrected. Infrared (IR) spectra were recorded on Mattson 5000 FT-IR spectrometer. ^{1}H NMR spectra were recorded on FT-NMR spectrometer (200 MHz) Gemini Varian and ^{13}C NMR on Ultra shield Bruker (125 MHz) using DMSO-d_6 and/or $CDCl_3$ and using TMS as internal standard (chemical shifts in δ ppm). Mass spectra were measured on JEOL JMS-600H spectrometer. Elemental analysis was carried out for C, H and N at the Microanalytical Centre of Cairo University. All reagents were purchased from the Aldrich Chemical Company. The well-known compounds, 1-(4-chlorophenyl)-4,4,4-trifuorobutane-1,3-dione (**1**),[18] 5-(4-chlorophenyl)-1-phenyl-3-(trifluoromethyl)-1*H*-pyrazole (**6**)[41,42] and 5-(4-chlorophenyl)-1-phenyl-3-(trifluoromethyl)-1*H*-pyrazole-4-carbaldehyde (**7**)[19] were prepared following the procedures reported in the literature.

4.2. General method for synthesis of 2-(2-arylidene)-1-(4-chloro phenyl)-4,4,4-trifuorobutane-1,3-dione (2a–f) (Scheme 1)

A mixture of compound **1** (2.50 g, 10 mmol) and the appropriate aldehyde (10 mmol) in ethanolic sodium hydroxide solution (5%, 40 mL) was refluxed for 2 h. The reaction mixture was poured onto ice/cold water and the formed precipitate was filtered off and recrystallized from ethanol to give compounds **2a**–**f**.

4.2.1. 1-(4-Chlorophenyl)-2-(2-hydroxybenzylidene)-4,4,4-trifluorobutane-1,3-dione (2a)

Yield, 70%; mp 110–111 °C; IR (KBr) ν_{max}/cm^{-1} 3328 (OH), 1650, 1589 (C=O). ^{1}H NMR (DMSO-d_6); δ 9.71 (br s, 1H, OH), 8.08–7.20 (m, 8H, Ar-H), 7.11 (s, 1H, =CH). Anal. Calcd for $C_{17}H_{10}ClF_3O_3$: C, 57.56; H, 2.84. Found: C, 57.43; H, 2.91.

4.2.2. 1-(4-Chlorophenyl)-2-(4-hydroxybenzylidene)-4,4,4-trifluorobutane-1,3-dione (2b)

Yield, 60%; mp 120–121 °C; ^{1}H NMR (DMSO-d_6); δ 9.61 (br s, 1H, OH), 8.08–7.10 (m, 9H, Ar-H, =CH). Anal. Calcd for $C_{17}H_{10}ClF_3O_3$: C, 57.56; H, 2.84. Found: C, 57.30; H, 2.60.

4.2.3. 1-(4-Chlorophenyl)-2-(4-methoxybenzylidene)-4,4,4-trifluorobutane-1,3-dione (2c)

Yield, 55%; mp 90–92 °C; ^{1}H NMR (DMSO-d_6); δ 8.18–7.20 (m, 8H, Ar-H), 7.08 (s, 1H, =CH), 3.81 (s, 3H, OCH_3). ^{13}C NMR ($CDCl_3$): δ 191.18, 159.33, 138.98, 136.34, 134.06, 131.85, 129.71, 129.10, 128.58, 127.17, 118.75, 118.59, 115.25, 55.67. Anal. Calcd for $C_{18}H_{12}ClF_3O_3$: C, 58.63; H, 3.28. Found: C, 58.35; H, 3.10.

4.2.4. 1-(4-Chlorophenyl)-2-(3,4-dimethoxybenzylidene)-4,4,4-trifluorobutane-1,3-dione (2d)

Yield, 60%; mp 105–107 °C; IR (KBr) ν_{max}/cm^{-1} 1645, 1595 (C=O). ^{1}H NMR (DMSO-d_6); δ 8.20–7.00 (m, 8H, Ar-H, =CH), 3.90 (s, 3H, OCH_3), 3.80 (s, 3H, OCH_3). ^{13}C NMR (DMSO): δ 187.89, 151.41, 148.98, 145.06, 137.83, 136.47, 130.33, 128.80, 128.47, 127.36, 124.17, 119.18, 111.51, 55.71, 55.57. MS *m/z* (%); 399.00 (1.72, M^++1), 398.00 (1.77, M^+), 302.00 (100.00), 160.05 (0.83), 158.00 (2.10), 109.05 (1.26), 107.05 (3.36). Anal. Calcd for $C_{19}H_{14}ClF_3O_4$: C, 57.23; H, 3.54. Found: C, 57.00; H, 3.20.

4.2.5. 1-(4-Chlorophenyl)-2-(3-nitrobenzylidene)-4,4,4-trifluorobutane-1,3-dione (2e)

Yield, 60%; mp 125–127 °C; ^{1}H NMR (DMSO-d_6); δ 8.18–7.10 (m, 9H, =CH, Ar-H). Anal. Calcd for $C_{17}H_9ClF_3NO_4$: C, 53.21; H, 2.36; N, 3.65. Found: C, 53.00; H, 2.10; N, 3.30.

4.2.6. 1-(4-Chlorophenyl)-2-((furan-2-yl)methylene)-4,4,4-trifluorobutane-1,3-dione (2f)

Yield, 55%; mp 130–131 °C; ^{1}H NMR ($CDCl_3$); δ 8.40–6.80 (m, 8H, Ar-H, furyl-H, =CH). MS *m/z* (%); 328.00 (37.78, M^+), 327.00 (32.94), 264.00 (32.25), 246.00 (100.00), 168.00 (30.25) 82.00

(44.45). Anal. Calcd for $C_{15}H_8ClF_3O_3$: C, 54.81; H, 2.45. Found: C, 54.51; H, 2.15.

4.3. General method for synthesis of 3,4,5-trisubstituted pyrazole derivatives (3a–f) (Scheme 1)

A mixture of chalcone derivatives **2a–f** (3 mmol) and hydrazine hydrate (0.32 g, 3 mmol) in absolute ethanol (30 mL) was refluxed for 3–6 h. Upon cooling, the obtained product was filtered off and recrystallized from ethanol to give compounds **3a–f**.

4.3.1. 2-((3-(4-Chlorophenyl)-5-(trifluoromethyl)-4*H*-pyrazol-4-ylidene)methyl)phenol (3a)

Yield, 60%; mp 109–110 °C; IR (KBr) ν_{max}/cm^{-1} 3340 (OH), 1600, 1589 (C=N). ^1H NMR (DMSO-d_6); δ 9.71 (br s, 1H, OH exchangable with D_2O), 8.18–7.20 (m, 8H, Ar-H), 6.15 (s, 1H, =CH). Anal. Calcd for $C_{17}H_{10}ClF_3N_2O$: C, 58.22; H, 2.87; N, 7.99. Found: C, 58.10; H, 2.57; N, 8.11.

4.3.2. 4-((3-(4-Chlorophenyl)-5-(trifluoromethyl)-4*H*-pyrazol-4-ylidene)methyl)phenol (3b)

Yield, 65%; mp 123–125 °C; ^1H NMR (DMSO-d_6); δ 9.80 (br s, 1H, OH exchangable with D_2O), 8.18–7.10 (m, 9H, Ar-H =CH). ^{13}C NMR ($CDCl_3$): δ 164.12, 144.87, 141.23, 140.99, 136.77, 130.00, 127.56, 126.05, 124.69, 122.07, 119.33, 117.01. Anal. Calcd for $C_{17}H_{10}ClF_3N_2O$: C, 58.22; H, 2.87; N, 7.99. Found: C, 58.00; H, 2.99; N, 8.13.

4.3.3. 3-(4-Chlorophenyl)-4-(4-methoxybenzylidene)-5-(trifluoromethyl)-4*H*-pyrazole (3c)

Yield, 45%; mp 110–111 °C; ^1H NMR ($CDCl_3$); δ 8.22–7.30 (m, 8H, Ar-H), 7.18 (s, 1H, =CH), 3.75 (s, 3H, OCH_3). ^{13}C NMR ($CDCl_3$): δ 162.00, 143.29, 142.70, 142.40, 134.51, 128.53, 125.85, 125.38, 123.08, 120.94, 118.80, 116.66, 62.40. Anal. Calcd for $C_{18}H_{12}ClF_3N_2O$: C, 59.27; H, 3.32; N, 7.68. Found: C, 59.53; H, 3.12; N, 7.93.

4.3.4. 3-(4-Chlorophenyl)-4-(3,4-dimethoxybenzylidene)-5-(trifluoromethyl)-4*H*-pyrazole (3d)

Yield, 60%; mp 105–107 °C; ^1H NMR (DMSO-d_6); δ 7.70–7.03 (m, 7H, Ar-H), 6.93 (s, 1H, =CH), 3.75 (s, 3H, OCH_3), 3.62 (s, 3H, OCH_3). Anal. Calcd for $C_{19}H_{14}ClF_3N_2O_2$: C, 57.81; H, 3.57; N, 7.10. Found: C,57.62; H, 3.32; N, 7.31.

4.3.5. 3-(4-Chlorophenyl)-4-(3-nitrobenzylidene)-5-(trifluoromethyl)-4*H*-pyrazole (3e)

Yield, 55%; mp 98–99 °C; ^1H NMR (DMSO-d_6); δ 8.18–7.10 (m, 9H, =CH, Ar-H). Anal. Calcd for $C_{17}H_9ClF_3N_3O_2$: C, 53.77; H, 2.39; N, 11.07. Found: C, 53.52; H, 2.15; N, 11.31.

4.3.6. 3-(4-Chlorophenyl)-4-((furan-2-yl)methylene)-5-(trifluoromethyl)-4*H*-pyrazole (3f)

Yield, 55%; mp 96–98 °C; ^1H NMR ($CDCl_3$); δ 8.50-6.70 (m, 8H, Ar-H, furyl-H, =CH). MS *m/z* (%); 324.60 (10.14, M^+), 262.15 (9.90), 245.95 (100.00), 136.70 (15.46), 82.45 (10.85) 68.20 (15.59). Anal. Calcd for $C_{15}H_8ClF_3N_2O$: C, 55.49; H, 2.48; N, 8.63. Found: C, 55.21; H, 2.22; N, 8.32.

4.4. General method for synthesis of 2-benzyl-1-(4-chlorophenyl)-4,4,4-trifluorobutane-1,3-dione (4) (Scheme 1)

To a stirred solution of compound 1 (0.25 g, 1 mmol) and benzyl alcohol (0.10 g, 1 mmol) in dry dichloromethane (4 mL) was added anhydrous ferric chloride (0.16 g, 0.1 mmol). The mixture was refluxed for 3 h. The reaction mixture was evaporated under reduced pressure and the residue was crystallized from isopropanol to give compound **4**. Yield, 40%; mp 90–91 °C; ^1H NMR ($CDCl_3$); δ 7.81–7.40 (m, 9H, Ar-H), 3.8 (t, 1H, CH), δ 3.2 (d, 2H, CH_2, J = 7.5 Hz). Anal. Calcd for $C_{17}H_{12}ClF_3O_2$: C, 59.93; H, 3.55. Found: C, 60.10; H, 3.83.

4.5. General method for synthesis of 4-benzyl-3-(4-chlorophenyl)-5-(trifluoromethyl)-1*H*-pyrazole (5) (Scheme 1)

A mixture compound **4** (1.02 g, 3 mmol) and hydrazine hydrate (0.32 g, 3 mmol) in absolute ethanol (30 mL) was refluxed for 6 h. The reaction mixture was evaporated under reduced pressure and the residue was crystallized from chloroform to give compound **5**. Yield, 50%; mp 148–150 °C; IR (KBr) ν_{max}/cm^{-1} 3200, 3096 (NH), 1610, 1590 (C=C, C=N) ^1H NMR ($CDCl_3$); δ 14.10 (s, 1H, NH), 7.86–7.27 (m, 9H, Ar-H), 4.2 (s, 2H, CH_2). Anal. Calcd for $C_{17}H_{12}ClF_3N_2$: C, 60.64; H, 3.59; N, 8.32. Found: C, 60.35; H, 3.81; N, 8.62.

4.6. General method for synthesis of *N*-((5-(4-chlorophenyl)-1-phenyl-3-(trifluoromethyl)-1*H*-pyrazol-4-yl)methylene)aniline derivatives (8a–d) (Scheme 2)

To a mixture of compound **7** (17.53 g, 0.05 mol) and the appropriate aromatic aldehyde (0.05 mol) in absolute ethanol (20 mL), glacial acetic acid (0.5 mL) was added and the reaction mixture was refluxed for 5 h. The resulting clear solution was evaporated under reduced pressure and the residue was crystallized from aqueous ethanol to give compounds **8a–d**.

4.6.1. 4-Bromo-*N*-((5-(4-chlorophenyl)-1-phenyl-3-(trifluoromethyl)-1*H*-pyrazol-4-yl)methylene)aniline (8a)

Yield, 80%; mp 125–126 °C; ^1H NMR ($CDCl_3$); δ 7.95–7.40 (m, 14H, CH=N, Ar-H). ^{13}C NMR ($CDCl_3$): δ 184.45, 153.21, 145.03, 141.11, 138.91, 135.45, 132.00, 131.12, 130.20, 129.86, 129.75, 128.95, 128.13, 126.32, 122.53, 120.57, 119.75. MS *m/z* (%); 505.00 (0.71, M^+), 504.00 (0.57), 360.40 (0.78), 358.20 (0.80), 150.00(100.00), 144.05 (3.50), 142.00 (3.60). Anal. Calcd for $C_{23}H_{14}BrClF_3N_3$: C, 54.73; H, 2.80; N, 8.33. Found: C, 55.00; H, 2.61; N, 8.60.

4.6.2. 2-Chloro-*N*-((5-(4-chlorophenyl)-1-phenyl-3-(trifluoromethyl)-1*H*-pyrazol-4-yl)methylene)aniline (8b)

Yield, 85%; mp 139–140 °C; ^1H NMR ($CDCl_3$); δ 7.83–7.52 (m, 14H, CH=N, Ar-H). ^{13}C NMR ($CDCl_3$): δ 184.45, 153.21, 145.00, 141.00, 138.91, 135.44, 132.07, 130.20, 129.86, 129.74, 128.93, 128.11, 126.30, 122.52, 120.31, 119.73. Anal. Calcd for $C_{23}H_{14}Cl_2F_3N_3$: C, 60.02; H, 3.07; N, 9.13. Found: C, 60.33; H, 3.30; N, 9.35.

4.6.3. *N*-((5-(4-chlorophenyl)-1-phenyl-3-(trifluoromethyl)-1*H*-pyrazol-4-yl)methylene)-4-nitroaniline (8c)

Yield, 75%; mp 235–237 °C; ^1H NMR ($CDCl_3$); δ 7.81–7.40 (m, 14H, CH=N, Ar-H). Anal. Calcd for $C_{23}H_{14}ClF_3N_4O_2$: C, 58.67; H, 3.00; N, 11.90. Found: C, 58.89; H, 3.30; N, 12.10.

4.6.4. 3,5-bi(Trifluoromethyl)-*N*-((5-(4-chlorophenyl)-1-phenyl-3-(trifluoromethyl)-1*H*-pyrazol-4-yl)methylene)aniline (8d)

Yield, 80%; mp 235–237 °C; ^1H NMR ($CDCl_3$); δ 7.80–7.45 (m, 13H, CH=N, Ar-H). ^{13}C NMR ($CDCl_3$): δ 184.45, 153.20, 145.11, 141.21, 138.91, 135.45, 132.01, 131.11, 130.20, 129.85, 129.75, 128.94, 128.13, 126.81, 122.53, 120.44, 119.75, 118.51. Anal. Calcd for $C_{25}H_{13}ClF_9N_3$: C, 53.44; H, 2.33; N, 7.48. Found: C, 53.75; H, 2.00; N, 7.55.

4.7. General method for synthesis of 2-(5-(4-chlorophenyl)-1-phenyl-3-(trifluoromethyl)-1*H*-pyrazol-4-yl)methylene)-malononitrile (9) (Scheme 2)

A mixture of compound **7** (1.75 g, 0.005 mol), malononitril (0.30 g, 0.005 mol) and sodium acetate (3.28 g, 0.04 mol) in absolute ethanol (30 mL) was refluxed for 10 h. The solvent was evaporated under reduced pressure and the residue obtained was triturated with water, filtered and dried to give compound **9** which crystallized DMF/water.

Yield, 40%; mp 105–110 °C; IR (KBr) ν_{max}/cm^{-1} 2211,2205 (CN), 1579 (C=N). ^1H NMR ($CDCl_3$); δ 8.00–7.10 (m, 10H, CH=C, Ar-H). ^{13}C NMR ($CDCl_3$): d 163.12, 138.21, 137.35, 136.00, 132.50, 129.89, 129.50, 129.07, 128.90, 128.51, 126.11, 116.00, 113.11, 100.00, 90.21. MS m/z (%); 399.00 (1.72, M_++1), 398.00 (1.77, M_+), 302.95(35.98), 302.00 (100.00), 271.00 (42.35), 139.00 (29.39), 111.00 (22.13). Anal. Calcd for $C_{20}H_{10}ClF_3N_4$: C, 60.24; H, 2.53; N, 14.05. Found: C, 60.00; H, 2.70; N, 14.20.

4.8. General method for synthesis of 5′-(4-substituted phenyl)-5-fluoro-2′,4′-dihydrospiro(indol-3,3′-pyrazol)-2(1*H*)-one 11a,b (Scheme 3)

To a mixture of fluoroisatin (0.82 g, 5 mmol) and acetophenone derivatives (5 mmol), dimethylamine (5 drops) was added and the mixture was stirred for 30 min at room temperature. To the formed solid, glacial acetic acid (10 mL) and concentrated hydrochloric acid (3 drops) were added and the reaction mixture was heated at 80 °C for 30 min. Hydrazine hydrate (6 mmol) was added to the previous reaction mixture and heating was continued at 80 °C for 1 h to give spiro compounds **11a,b** which crystallized from DMF.

4.8.1. 5′-(4-Bromophenyl)-5-fluoro-2′,4′-dihydrospiro(indol-3,3′-pyrazol)-2(1*H*)-one (11a)

Yield, 45%; mp 120–122 °C; IR (KBr) ν_{max}/cm^{-1} 3210, 3087 (NH), 1706 (C=O), 1587 (C=N). ^1H NMR (DMSO-d_6); δ 10.2 (s, 1H, NH), 7.85–7.01 (m, 7H, Ar-H), 6.6 (s, 1H, NH), 3.5 (d, 2H, CH_2, J = 15.0 Hz). ^{13}C NMR (DMSO): δ 167.04, 156.97,139.92, 137.93, 137.21, 135.72, 131.43, 129.98, 127.72, 125.71, 123.80, 120.52, 62.92, 50.00. MS *m/z* (%); 359.75 (5.62, M^+), 358.00 (48.59), 356.05 (33.66), 350.55 (43.64), 348.65 (46.40), 236.10 (100.00), 92.55 (11.10), 90.30 (13.21). Anal. Calcd for $C_{16}H_{11}BrFN_3O$: C, 53.35; H, 3.08; N, 11.67. Found: C, 53.80; H, 3.20; N, 11.92.

4.8.2. 5′-(4-Methylphenyl)-5-fluoro-2′,4′-dihydrospiro(indol-3,3′-pyrazol)-2(1*H*)-one (11b)

Yield, 50%; mp 142–143 °C; IR (KBr) ν_{max}/cm^{-1} 3417, 3031 (NH), 1600 (C=O), 1562 (C=N). ^1H NMR (DMSO-d_6); δ 11.0 (s, 1H, NH), 7.75–7.00 (m, 7H, Ar-H), 6.8 (s, 1H, NH), 3.5 (d, 2H, CH_2, J = 15.1 Hz), 2.5(s, 3H, CH_3). ^{13}C NMR (DMSO): δ 172.00, 157.41,139.36, 137.24, 135.24, 130.00, 129.63, 129.45, 128.96, 126.55, 126.89, 124.00, 63.00, 50.00, 20.87. MS *m/z* (%); 294.00 (50.62, M^+-H), 278.10 (100.00), 277.05 (52.29), 132.25 (57.03), 129.45 (63.46), 111.75(62.19). Anal. Calcd for $C_{17}H_{14}FN_3O$: C, 69.14; H, 4.78; N, 14.23. Found: C, 69.40; H, 4.95; N, 14.61.

5. Biological evaluation

5.1. In vitro cyclooxygenase (COX) inhibition assay

The ability of the test compounds to inhibit ovine COX-1 and COX-2 was determined using an enzyme immuno assay (EIA) (Catalog No. 560101, Cayman chemicals, Ann Arbor, MI) according to our previous reports.[15,19]

5.2. Anti-inflammatory experiment

The anti-inflammatory activity was evaluated using in vivo rat carrageenin-induced foot paw edema model reported previously.[15,19]

6. Molecular modeling methods

6.1. 2D-descriptor calculations

6.1.1. Data set

A data set of 20 compounds was used for the present 2D QSAR study. There is high structural diversity and a sufficient range of the biological activity in the selected series of these derivatives. The biological activity values (IC_{50}) were converted to negative logarithmic scale ($-\log 1/IC_{50}$) and subsequently used as the dependent variable for the QSAR analysis. The energy-minimized geometry of the compounds was used for the calculation of the various 2D descriptors (Individual, Chi, ChiV, Path count, ChiChain, ChiVChain, Chainpathcount, Cluster, Pathcluster, Kapa, Element Count, Estate number, Estate contribution, Hydophillic–hydophobic and Polar surface area). The various alignment-independent (AI) descriptors were also calculated. For calculation of alignment, the independent descriptor was assigned the utmost three attributes. The first attribute was T to characterize the topology of the molecule. The second attribute was the atom type, and the third attribute was assigned to atoms taking part in the double or triple bond. The pre-processing of the independent variables (i.e., 2D descriptors) was done by removing invariable (constant column).

6.1.2. Statistical analysis

The descriptors were taken as independent variables and COX-2 inhibition as dependent variable. Multiple linear regression (MLR) method of analysis was used to derive the 2D QSAR equations. The developed QSAR models are evaluated using the following statistical measures: r^2, (the squared correlation coefficient); r^2se, (standard error of squared correlation coefficient); F test, (Fischer's value) for statistical significance; q^2, (cross-validated correlation coefficient); q^2_se, (standard error of cross-validated square correlation co-efficient); pred_r^2, (r^2 for external test set); pred_r^2se, (standard error of predicted squared regression); Z score, (Z score calculated by the randomization test); best_ran_q^2, (highest q^2 value in the randomization test). The regression coefficient r^2 is a relative measure of fit by the regression equation. It represents the part of the variation in the observed data that is explained by the regression. However, a QSAR model is considered to be predictive, if the following conditions are satisfied: r^2 >0.6, q^2 >0.6 and pred_r^2 >0.5.[43,44] The F-test reflects the ratio of the variance explained by the model and the variance due to the error in the regression. High values of the F-test indicate that the model is statistically significant. The low standard error of r^2 (r^2_se), q^2 (q^2_se) and pred_r^2 (Pred_r^2se) shows absolute quality of fitness of the model.

6.2. Docking methodology

Docking studies have been performed using MOE 2008.10.[35] With this purpose, crystal structure of both COX-2/SC-558 (a selective inhibitor) and COX-1/flurbiprofen (a non-selective-inhibitor) complexes (PDB codes: 6COX and 1EQH, respectively) was obtained from the Protein Data Bank in order to prepare both proteins for docking studies. Docking procedure was followed using the standard protocol implemented in MOE 2008.10 and the geometry of resulting complexes was studied using the MOE's Pose Viewer utility.

Acknowledgments

The authors extend their appreciation to the Deanship of Scientific Research at King Saud University for funding the work through the research group Project No. RGP-VPP-163. The authors wish to express gratitude to V-life Science Technologies Pvt. Ltd for providing the trial full version software. Our sincere acknowledgments to Chemical Computing Group Inc., 1010 Sherbrooke Street West, Suite 910, Montreal, H3A 2R7, Canada, for its valuable agreement to use the package of MOE 2008.10 software.

Supplementary data

Supplementary data associated with this article can be found, in the online version, at http://dx.doi.org/10.1016/j.bmc.2012.03.044.

References and notes

1. Williams, D. A.; Lemke, T. L. Non-steroidal anti-inflammatory drugs. In *Foye's Principles of Medicinal Chemistry*; Lippincott: Williams & Wilkins, 2002; pp 751–793. 5th ed.
2. Dannhardt, G.; Kiefer, W.; Krämer, G.; Maehrlein, S.; Nowe, U.; Fiebich, B. *Eur. J. Med. Chem.* **2000**, *35*, 499.
3. Dubost, J. J.; Soubrier, M.; Sauvezie, B. *Rev. Med. Intern.* **1999**, *20*, 171.
4. Frank, M. M.; Fries, L. F. *Immunol. Today* **1991**, *322*, 12.
5. Collier, H. O. J. *Nature* **1971**, *17*, 232.
6. Cryer, B.; Feldman, M. *Arch. Intern. Med.* **1992**, *152*, 1145.
7. Dannhardt, G.; Kiefer, W. *Eur. J. Med. Chem.* **2001**, *36*, 109.
8. Bayly, C. I.; Black, C.; Leger, S.; Ouimet, N.; Ouellet, M.; Percival, M. D. *Bioorg. Med. Chem. Lett.* **1999**, *9*, 307.
9. Vane, J. R. *Nat. New Biol.* **1971**, *231*, 232.
10. Buttar, N. S.; Wang, K. K. *Mayo Clin. Proc.* **2000**, *75*, 1027.
11. Michaux, C.; Charlier, C. *Mini Rev. Med. Chem.* **2004**, *4*, 603.
12. Patel, C. K.; Rami, C. S.; Panigrahi, B.; Patel, C. N. *J. Chem. Pharm. Res.* **2010**, *2*, 73.
13. Sakya, S. M.; Lundy DeMello, K. M.; Minich, M. L.; Rast, B.; Shavnya, A.; Rafka, R. J.; Koss, D. A.; Cheng, H.; Li, J.; Jaynes, B. H.; Ziegler, C. B.; Mann, D. W.; Petras, C. F.; Seibel, S. B.; Silvia, A. M.; George, D. M.; Lund, L. A.; Denis, S. St.; Hickman, A.; Haven, M. L.; Lynch, M. P. *Bioorg. Med. Chem. Lett.* **2006**, *16*, 288.
14. Lehman, F. S.; Beglinger, C. *Curr. Top. Med. Chem.* **2005**, *5*, 449.
15. Abdel-Aziz, A. A.-M.; ElTahir, K. E. H.; Asiri, Y. A. *Eur. J. Med. Chem.* **2011**, *46*, 1648.
16. Chakraborti, A. K.; Garg, S. K.; Kumar, R.; Motiwala, H. F.; Jadhavar, P. S. *Curr. Med. Chem.* **2010**, *17*, 1563.
17. Wang, J. L.; Limburg, D.; Graneto, M. J.; Springer, J.; Hamper, J. R. B.; Liao, S.; Pawlitz, J. L.; Kurumbail, R. G.; Maziasz, T.; Talley, J. J.; Kiefer, J. R.; Carter, J. *Bioorg. Med. Chem. Lett.* **2010**, *20*, 7159.
18. Penning, T. D.; Talley, J. J.; Bertenshaw, S. R.; Carter, J. S.; Collins, P. W.; Docter, S.; Graneto, M. J.; Lee, L. F.; Malecha, J. W.; Miyashiro, J. M.; Rogers, R. S.; Rogier, D. J.; Yu, S. S.; Anderson, G. D.; Burton, E. G.; Cogburn, J. N.; Gregory, S. A.; Koboldt, C. M.; Perkins, W. E.; Seibert, K.; Veenhuizen, A. W.; Zhang, Y. Y.; Isakson, P. C. *J. Med. Chem.* **1997**, *40*, 1347.
19. El-Sayed, M. A.-A.; Abdel-Aziz, N. I.; Abdel-Aziz, A. A.-M.; El-Azab, A. S.; Asiri, Y. A.; ElTahir, K. E. H. *Bioorg. Med. Chem.* **2011**, *19*, 3416.
20. Jana, U.; Biswas, S.; Maiti, S. *Tetrahedron Lett.* **2007**, *48*, 4065.
21. Das, N.B.; Mittra, A.S. Ind. J. Chem. 1978, 16b, 638.
22. Azarifar, D.; Shaebanzadeh, M. *Molecules* **2002**, *7*, 885.
23. Le'vai, A. *J. Heterocycl. Chem.* **2002**, *39*, 1.
24. Levai, A. *ARKIVOC* **2005**, *iv*, 344.
25. Azizian, J.; Shaebanzadeh, M.; Hatamjafari, F.; Mohammadizadeh, M. R. *ARKIVOC* **2006**, *xi*, 47.
26. McGettigan, P.; Henry, D. *JAMA* **2006**, *296*, 1633.
27. El-Ayaan, U.; Abdel-Aziz, A. A.-M.; Al-Shihry, S. *Eur. J. Med. Chem.* **2007**, *42*, 1325.
28. Goda, F. E.; Abdel-Aziz, A. A.-M.; Ghoneim, H. A. *Bioorg. Med. Chem.* **2005**, *13*, 3175.
29. Lipinski, C. A.; Lombardo, F.; Dominy, B. W.; Feeney, P. J. *Adv. Drug Deliv. Rev.* **2001**, *46*, 3.
30. V-Life Molecular Design Suite 3.5, VLife Sciences Technologies Pvt. Ltd; www.Vlifesciences.com.
31. Meade, E. A.; Smith, W. L.; DeWitt, D. L. *J. Biol. Chem.* **1993**, *268*, 6610.
32. Kurumbail, R. G.; Stevens, A. M.; Gierse, J. K.; McDonald, J. J.; Stegemen, R. A.; Pak, J. Y.; Gildehaus, D.; Miyashiro, J. M.; Penning, T. D.; Seibert, K.; Isakson, P. C.; Stallings, W. C. *Nature* **1996**, *384*, 644.
33. Llorens, O.; Perez, J. L.; Palomer, A.; Mauleon, D. *Bioorg. Med. Chem. Lett.* **1999**, *9*, 2779.
34. Garavito, R. M.; DeWitt, D. L. *Biochem. Biophys. Acta* **1999**, *1441*, 278.
35. MOE 2008.10 of Chemical Computing Group. Inc.
36. El-Azab, A. S.; Al-Omar, M. A.; Abdel-Aziz, A. A.-M.; Abdel-Aziz, N. I.; El-Sayed, M. A.-A.; Aleisa, A. M.; Sayed-Ahmed, M. M.; Abdel-Hamide, S. G. *Eur. J. Med. Chem.* **2010**, *45*, 4188.
37. Halgren, T. A. *J. Comp. Chem.* **1996**, *17*, 490.
38. Sondhi, S. M.; Rani, R.; Roy, P.; Agrawal, S. K.; Saxena, A. K. *Bioorg. Med. Chem Lett.* **2009**, *19*, 1534.
39. Lima, L. M.; Castro, P.; Machado, A. L.; Fraga, C. A. M.; Lugnier, C.; Concalves de Moraes, V. L.; Barreiro, E. J. *Bioorg. Med. Chem.* **2002**, *10*, 3067.
40. Selinsky, B. S.; Gupta, K.; Sharkey, C. T.; Loll, P. J. *Biochemistry* **2001**, *40*, 5172.
40. Fustero, S.; Román, R.; Sanz-Cervera, J. F.; SimÓn-Fuentes, A.; Cuñat, A. C.; Villanova, S.; Murgu, M. *J. Org. Chem.* **2008**, *73*, 3523.
42. Singh, S. P.; Kumar, V.; Aggarwal, R. *J. Heterocycl. Chem.* **2006**, *43*, 1003.
43. Abdel-Aziz, A. A.-M.; Asiri, Y. A.; Al-Agamy, M. H. M. *Eur. J. Med. Chem.* **2011**, *46*, 5487.
44. Golbraikh, A.; Tropsha, A. *J. Mol. Graph. Model.* **2002**, *20*, 269.